Japanese Journal of Radiology (2020) 38:1158–1168
https://doi.org/10.1007/s11604-020-01024-1

ORIGINAL ARTICLE

An analysis of anatomical variations of the left pulmonary artery of the interlobar portion for lung resection by three-dimensional CT pulmonary angiography and thin-section images

Makiko Murota[1] · Yuka Yamamoto[1] · Katashi Satoh[2] · Mariko Ishimura[1] · Naoya Yokota[3] · Takashi Norikane[1] · Katsuya Mitamura[1] · Yasukage Takami[1] · Kengo Fujimoto[1] · Yoshihiro Nishiyama[1]

Received: 22 February 2020 / Accepted: 21 July 2020 / Published online: 29 July 2020

Abstract

Purpose The purpose of the present study was to analyze the left pulmonary artery (LPA) branching pattern of the interlobar portion using three-dimensional CT pulmonary angiography (3D-CTPA) and thin-section CT images, and to attempt to diagrammatize these patterns.

Materials and methods The study included 320 patients suspected of having lung cancer of the left upper/lower lobe who underwent CTPA. The number and origin of the LPA branches of the interlobar portion, A1 + 2c, A6, and lingular artery from pars interlobaris (PI), were identified meticulously using 3D-CTPA and thin-section images. We then diagrammatized the identified LPA branching patterns of the interlobar portion.

Results The diagrammatized LPA branching patterns of the interlobar portion were broadly classified into seven types in the order of bifurcation from proximal to distal. Type 1 was the most frequent (120/320, 37.5%). PI originated from the lower portion, that is, from A8 or the common trunk of A8 and A9 in 95 cases (29.7%). We could also precisely diagrammatize the LPA branching patterns of the interlobar portion into 85 types in all 320 patients.

Conclusion 3D-CTPA and thin-section images provided precise preoperative information regarding the LPA branching patterns of the interlobar portion.

Keywords Pulmonary arteries · Three-dimensional CT pulmonary angiography · Video-assisted thoracic surgery · Anatomy · Lung cancer

Introduction

Knowledge of the pulmonary artery (PA) branching pattern is essential, because surgeons occasionally encounter unexpected bleeding from the PA during pulmonary resection. Therefore, identification and appropriate management of the PA branches is considered a key to for successful anatomical pulmonary resection. Anatomic variations in the left PA (LPA) are far more common than in right PA [1, 2] and make lung resection more difficult especially when separation of the interlobar fissure is incomplete [3]. Thus, in this area, preoperative identification of the LPA branches of interlobar portion would greatly contribute to the patient safety and easiness of the lung resection.

Several reports have described the utilities of preoperative evaluation of PA using three-dimensional CT pulmonary angiography (3D-CTPA) [4–8]. Some investigators have reported that 3D-CTPA may increase the safety of surgical procedures, including video-assisted thoracic surgery (VATS) lobectomy and limited resection [4, 9–12]. Moreover, it is necessary to assess preoperative PA branching pattern not only by 3D-CTPA but also by the thin-section CT images in order to provide better evaluation of smaller PA branches [13]. To the best of our knowledge, the LPA branching pattern of the interlobar portion with 3D-CTPA

✉ Makiko Murota
mwada@med.kagawa-u.ac.jp

[1] Faculty of Medicine, Department of Radiology, Kagawa University, 1750-1 Ikenobe, Miki-cho, Kita-gun, Kagawa 761-0793, Japan

[2] Department of Radiology, Diagnostic Imaging Center, Utazu Hospital, Utazu-cho, Kagawa, Japan

[3] Faculty of Medicine, Department of General Thoracic Surgery, Kagawa University, Miki-cho, Kita-gun, Kagawa, Japan

and thin-section images has not been investigated. Therefore, we analyzed the LPA branching pattern of the interlobar portion using 3D-CTPA and thin-section CT images, and also attempted to diagrammatize the results.

Materials and methods

Patients

The Ethics Committee of our hospital approved this retrospective study and waived the need for obtaining the consent of individual patients. A total of 374 consecutive patients suspected of having lung cancer of the left upper/lower lobe, who underwent pulmonary angiography scans using multidetector row CT (MDCT) between August 2012 and August 2018, were retrospectively reviewed. Of these, 54 patients were excluded from this study because of technical problems, poor investigation of hilar structures involved by tumor, and previous left lung surgery. The final study population included 320 patients (186 men, 134 women; mean age, 69.7 years; age range, 22–92 years) (Fig. 1). Of these 320 patients, 261 underwent pulmonary resection (upper lobectomy in 99 patients, lower lobectomy in 59, upper division segmentectomy in 24, lingular segmentectomy in 12, basal segmentectomy in 7, S1 + 2 segmentectomy in 4, S3 segmentectomy in 2, S6 segmentectomy in 8, S8/S8 + 9 segmentectomy in 3, wedge resection in 38, pneumonectomy in 2, and others in 3), whereas 59 were inoperable case or underwent follow-up. In patients who had undergone anatomical resection, such as lobectomy/segmentectomy, postoperative complications were retrieved from available clinical records. The development of postoperative complications in the present study was defined as Grade 2 or above for severe complications under the Clavien–Dindo classification system [14].

Contrast-enhanced MDCT

A 64-slice MDCT (Aquilion 64, Toshiba Medical Systems, Tokyo, Japan) and a 256-slice MDCT (Brilliance iCT, Philips Healthcare, Cleveland, OH, USA) scanners were used. The technical parameters used for the 64-slice MDCT were as follows: a detector row configuration of 0.5 mm, a pitch of 53 (detector pitch 0.41), a reconstruction increment of 0.4 mm, and a section thickness of 0.5 mm. The corresponding values for the 256-slice MDCT were 0.625 mm, 53 (detector pitch 0.83), 0.5 mm, and 0.67 mm, respectively. An X-ray tube voltage of 120 kV and a current of 300 mA were used in all examinations. The examinations were performed with the patient in the supine position during a single breath-hold at end-inspiration.

A dual-head power injector (Dual Shot GX, Nemoto Kyorindo, Tokyo, Japan) was used for all patients for the bolus administration of the contrast material iohexol (Omnipaque 350, Daiichi-Sankyo, Tokyo, Japan) or iopamidol (Iopamiron 300, Bayer Yakuhin, Osaka, Japan) via a cubital vein. In patients weighing at least 55 kg, 100 ml of contrast medium iohexol (350 mg iodine/ml) was injected at a rate of 3.3 ml/s, and scanning was performed at 18 s after injection of the contrast medium. In patients with body weight from 44 kg–55 kg, 85 ml of contrast medium iohexol (350 mg iodine/ml) was injected at a rate of 3.3 ml/s, and scanning was performed at 15 s after injection of the contrast medium. In patients weighing less than 44 kg, 85 ml of contrast medium iopamidol (300 mg iodine/ml) was injected at a rate of 3.3 ml/s, and scanning was done at 15 s after injection of the contrast medium. There is one more protocol of PA and pulmonary vein (PV) separation images that was determined from the time–density curve (TDC) using a test bolus dose. The injection rate was 4 ml/s, with 20 ml test bolus injected prior to the main injection. The test injection determined the adequate timing for the PA/PV scan. The PA/PV scan was performed with 50 ml of contrast medium iohexol (350 mg iodine/ml). Saline chaser was 40 ml and injection rate was 4 ml/s. These two protocols were comparable to investigate PA branching pattern in detail. The volume data obtained from the arterial phase were transferred to a workstation (zio STATION, ziosoft, Tokyo, Japan), where the data were converted to a 3D-CTPA format using the volume-rendering technique.

Image analysis

Thin-section transverse images were reviewed at a width of 1600HU and level -200HU window settings with paging on a viewer (EV insite, PSP Corporation Corp., Tokyo, Japan). The 3D-CTPA images were interpreted by rotating on the same viewer. The window, level, and opacity of the volumes were subjectively selected to optimize visualization of the PA. In the present study, the number and origin of the LPA branches of the interlobar portion were identified meticulously using 3D-CTPA and thin-section images on the same viewer. These images were read with an interval of several days between interpretations. Two board-certified thoracic radiologists with 12 and 22 years of experience independently reviewed each CT image. When there was discrepancy over branching patterns between the investigators, the case was again reviewed with 3D-CTPA and thin-section images, and consensus was reached in order to avoid inter-observer variability. We then diagrammatized the identified LPA branching pattern of the interlobar portion. At first, the LPA branching patterns of the interlobar portion were broadly classified in the order of bifurcation from proximal to distal. Next, we diagrammatized more precisely the LPA

branching pattern of the interlobar portion. Figure 2 shows a 3D-CTPA image, a diagram of the LPA branching pattern of the interlobar portion identified by 3D-CTPA images, and intraoperative images of a 70-year-old man with lung cancer in the upper left lobe.

Anatomy

The nomenclature used to describe the segmental PA is that of Yamashita [15]. Regarding the LPA branching pattern of the interlobar portion, no one pattern for LPA may be described as standard, while a relatively typical distribution of the segmental arteries is often encountered. The branches to the left upper lobe arise from the anterior, posterosuperior, and interlobar portions of the vessel [1]. Yamashita described a prevailing pattern's schema of the left upper lobe arteries where the first branch A3, A1 + 2a, and A1 + 2b arises from the anterior portion of LPA [15]. The second branch, a separate posterior segmental branch (A1 + 2c), is found on the posterolateral surface of the interlobar portion on the main PA, just at or above the major fissure. The third branch, the superior segmental artery (A6), branches posteriorly to supply the superior segment of the lower lobe, and then the lingular artery originates from the interlobar portion (i.e., pars interlobaris) of PA distal to A6. The interlobar portion of the LPA is a part of the artery between the origin of the lowermost segmental branch to the upper lobe and its division into terminal branches to the lower lobe [16]. We defined the lingular artery as PI originating from the pars interlobaris, namely the interlobar portion of the LPA that passes to a site distal to the left upper lobe bronchus, and PM from the pars mediastinalis, the anterior portion of the mediastinal part of the left arterial trunk (Fig. 3). When anatomical resection is performed, dissection of the left major fissure demonstrates these PA branches (A1 + 2c, A6, and PI) of left interlobar portion. An important point to note in the branching pattern of the lingular arteries (A4 and A5) is that A4 and A5 may arise from pars mediastinalis in addition to pars interlobaris, and both or one of the lingular arteries arises from pars interlobaris with approximately 90% frequency [15]. Sometimes, the lingular arteries as PI originate from lower portion, from A8 or the common trunk of A8 and A9 [6]. Because some branches of upper lobe and lower lobe arise closely, the surgeon must be mindful of the high degree of variability of the branches of PA and carefully identify each branch before ligation.

In the present study, the number and origin of the LPA branches of the interlobar portion were identified as follows: A1 + 2c, the lingular arteries (A4 and A5), and A6. The lingular arteries are identified separately as PI and PI originated from lower portion, that is, from A8 or the common trunk of A8 and A9 (named as PI´). It was also noted that A3a arose from the posterolateral surface of the main LPA of the interlobar portion like A1 + 2c or from PI. Regarding the LPA branching pattern of the interlobar portion of "Yamashita's prevailing pattern," we defined as from A1 + 2c, a A6 to a PI in the order of bifurcation from the proximal to distal followed as his schema [15].

Results

Figures 4 and 5 show the diagrammatized LPA branching pattern of the interlobar portion: A1 + 2c, A6, and PI, according to the 3D-CTPA images and thin-section CT images. At first, the LPA branching patterns of the interlobar portion were broadly classified in the order of bifurcation from proximal to distal into seven types: Type 1––A1 + 2c, A6, and PI; Type 2—A6, A1 + 2c, and PI; Type 3—PI, A1 + 2c, and A6; Type 4—no A1 + 2c directly originated from the LPA of the interlobar portion; Type 5––no PI (lingular segment supplied solely from PM); Type 6––A3a directly originated from the LPA of the interlobar portion; Type 7—a few branches of A1 + 2c and/or A3a directly originated from the LPA of the interlobar portion, with frequencies of 37.5% (120/320), 13.1% (42/320), 0.9% (3/320), 31.0% (99/320), 4.7% (15/320), 5.9% (19/320), and 6.9% (22/320), respectively (Fig. 4). When there were several branches of A6 or PI, we determined the branch location by position of the most proximal branch. The cases with the same positions of A1 + 2c and A6 were classified as Type 2 and those with similar positions of PI and A1 + 2c were classified as Type 3. Among the seven broad classification types, Type 1 was the most

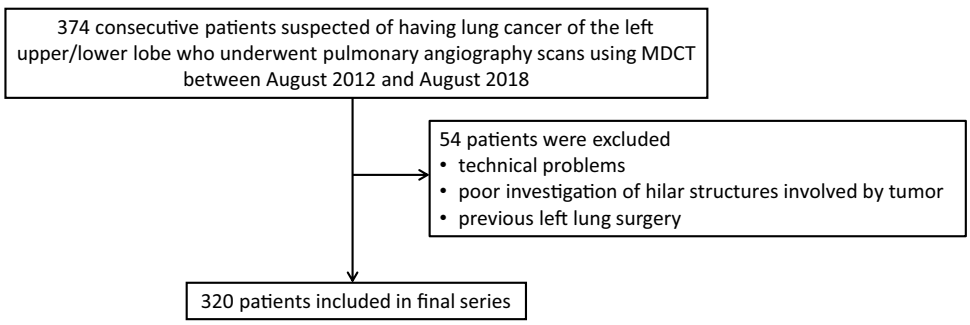

Fig. 1 Study flow chart

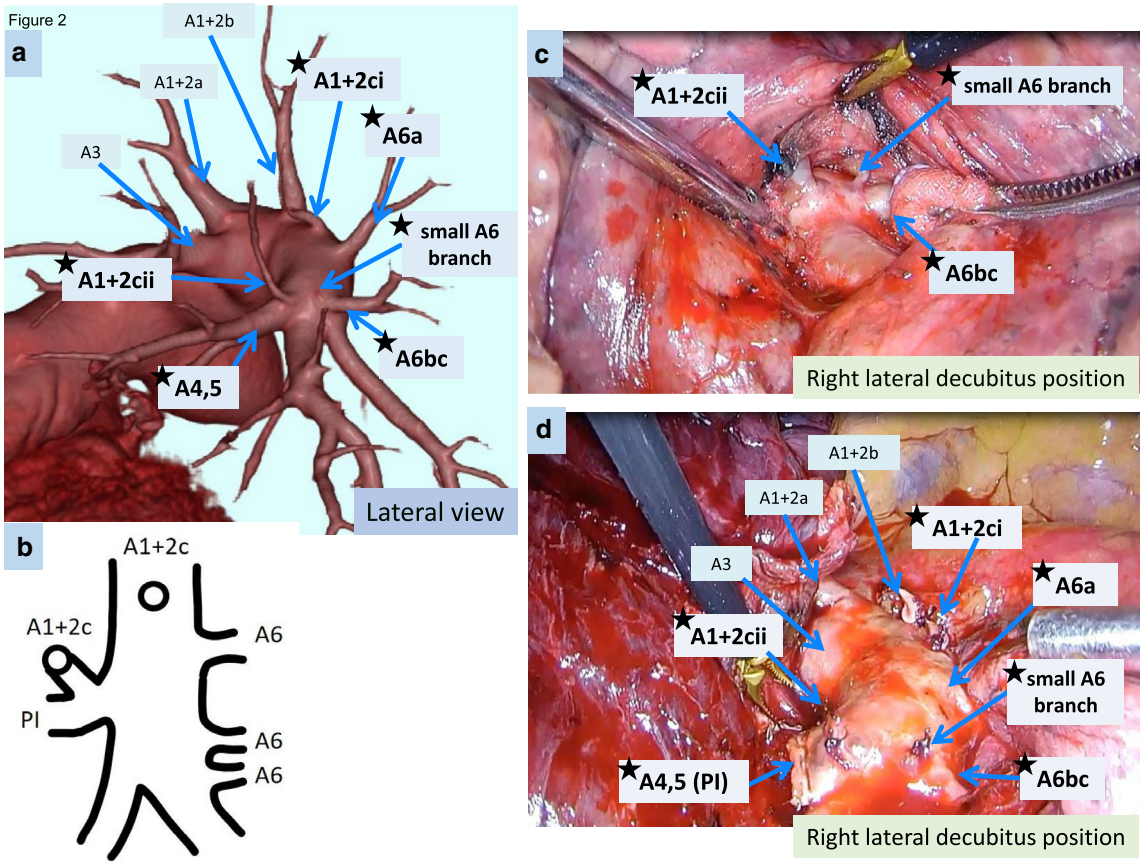

Fig. 2 3D-CTPA image, a diagram of the LPA branches of the interlobar portion identified by 3D-CTPA images, and the intraoperative images in a 70-year-old man with a lung cancer of left upper lobe. **a** 3D-CTPA image showing the branching pattern of left PA. **b** A diagram of the LPA branches of the interlobar portion identified by 3D-CTPA images. *PI* the lingular artery from pars interlobaris. **c**, **d** Intraoperative findings show Type 1 pattern with three A6 branches and another A1 + 2c from PI corresponding to the 3D-CTPA. In this case, small A6 branch was sacrificed to secure a field of view and avoid bleeding

frequent (120/320, 37.5%). Next, we could precisely diagrammatize the LPA branching pattern of the interlobar portion into 85 types in all 320 patients (Fig. 5).

Among the detailed the LPA branching patterns, "Yamashita's prevailing pattern" of the interlobar portion was seen in 48 cases (15.0%) and was the most common type.

PI´ was observed in 95 cases (29.7%).

In Type 7 of the broad classification types, the instances, where two branches of A1 + 2c directly originated from the LPA of the interlobar portion, were found in 15 cases (4.7%), where A1 + 2c and A3a directly originated from the LPA of the interlobar portion in 6 cases (1.9%), and where two branches of A1 + 2c and A3a directly originated from the LPA of the interlobar portion in one case (0.3%) (Fig. 5g).

A3a arose from PI in 26 cases (8.1%), A1 + 2c from PI (Fig. 2) in 12 cases (3.8%), A3a from A1 + 2c in 2 cases (0.6%), and A3a from A8 in one case (0.3%).

In three cases, four branches of A6 were seen. However, they were classified as three branches of A6, because one branch arose from the lower medial part of the interlobar PA in all three cases.

Fig. 3 Diagram of two types of branching pattern of lingular artery. ▶ **a** A diagram of anterior view and **b** A diagram of lateral view of the lingular artery that originates from pars interlobaris (PI, arrow). Lingular artery (A4,5) arises from the LPA of the interlobar portion that continues distal to the left upper lobe bronchus and into the interlobar fissure. **c** A diagram of anterior view and d a diagram of anterior view of the lingular artery that originates from pars mediastinalis (PM, arrowhead). Lingular artery (A4,5) arises from the anterior portion of mediastinal part of the left arterial trunk

In 218 patients who had undergone anatomical resection (lobectomy/segmentectomy), postoperative complications were occurred in 36 cases (16.5%) and there were no operative mortalities. Eight cases (3.7%) were converted from VATS to thoracotomy because of vascular bleeding.

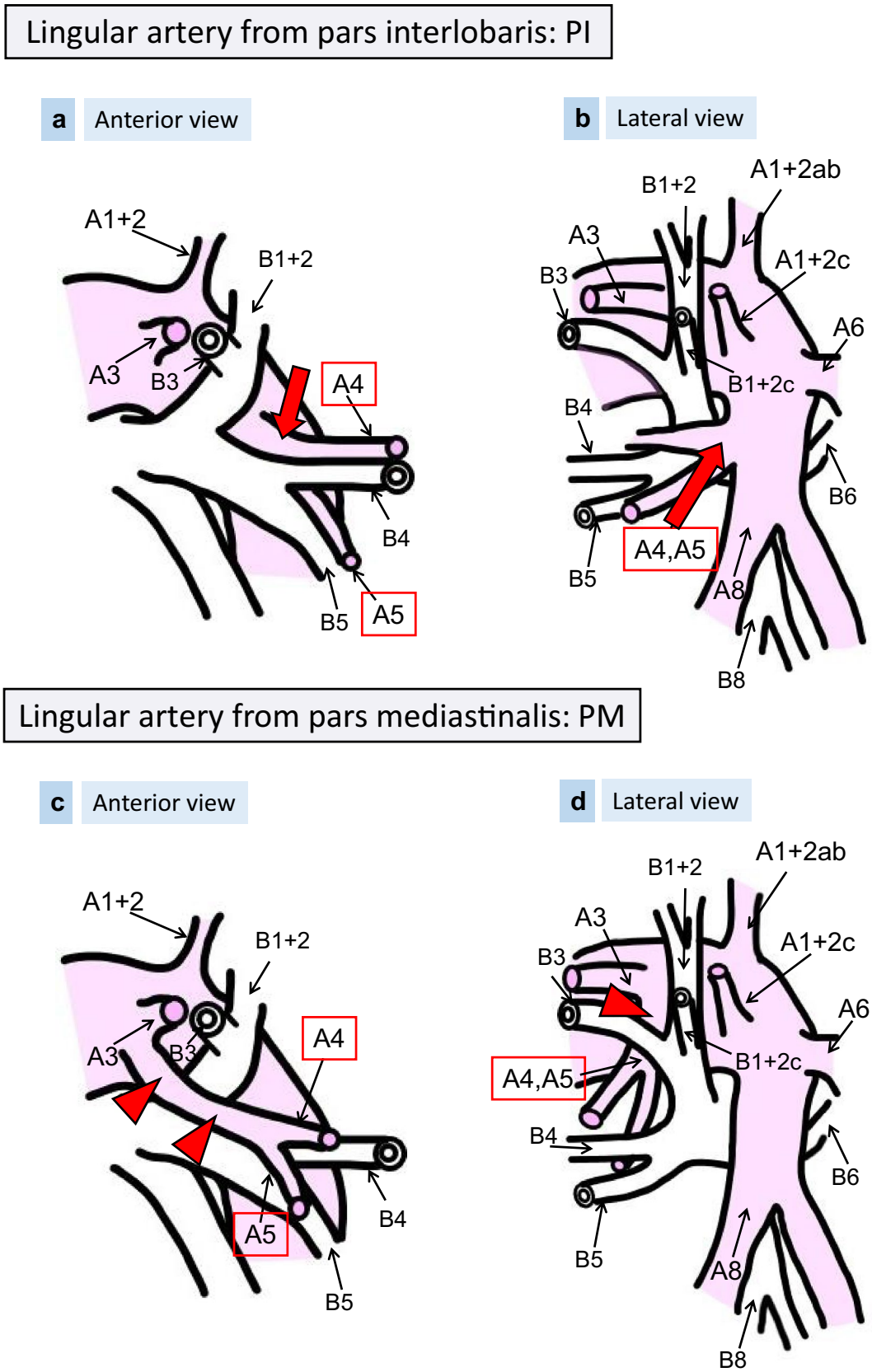
Lingular artery from pars interlobaris: PI
a Anterior view
A1+2
B1+2
A3
B3
A4
B4
B5
A5
b Lateral view
A1+2ab
B1+2
A3
B3
A1+2c
A6
B1+2c
B4
B6
A4,A5
B5
A8
B8
Lingular artery from pars mediastinalis: PM
c Anterior view
A1+2
B1+2
A3
B3
A4
A5
B4
B5
d Lateral view
A1+2ab
B1+2
A3
B3
A1+2c
A6
B1+2c
A4,A5
B4
B6
B5
A8
B8

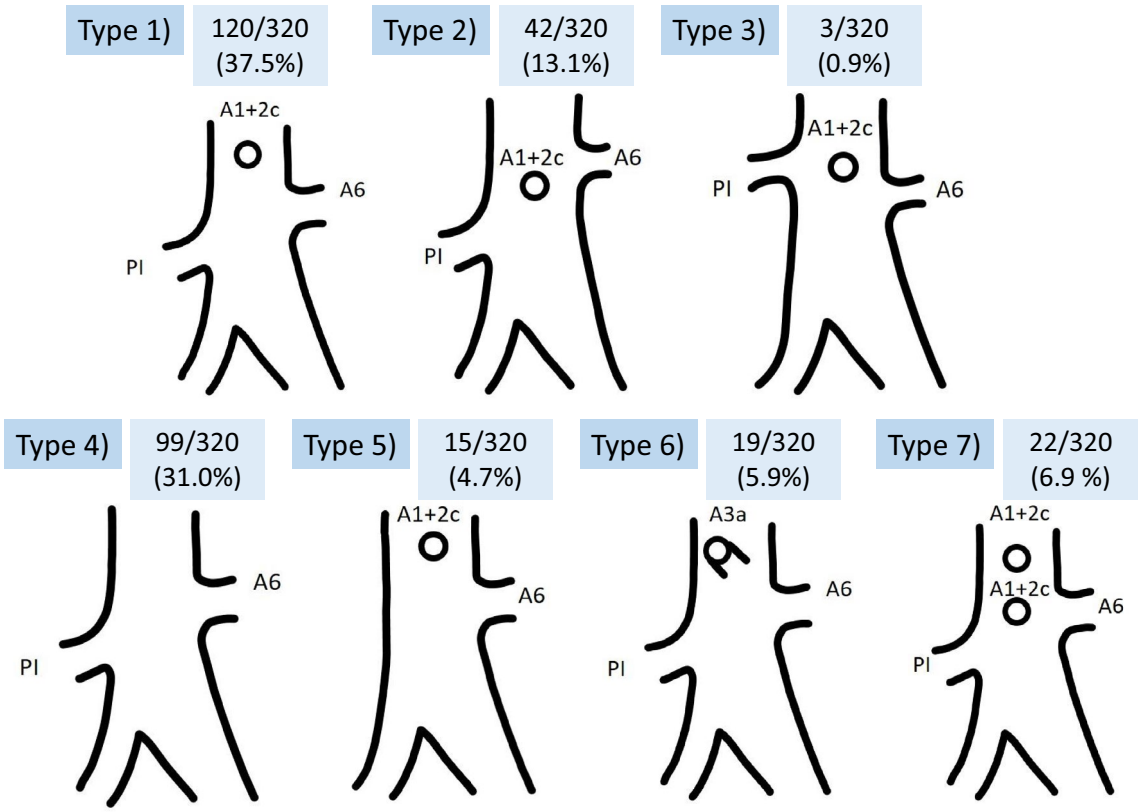

Fig. 4 Types of the LPA branching pattern of the interlobar portion: A broad classification schema. PI: the lingular artery from pars interlobaris

Discussion

The present study included a large number of subjects and analyzed the LPA branching pattern of the interlobar portion using 3D-CTPA and thin-section CT images. Although Yamashita examined the bronchovascular anatomy of 165 specimens [15], the study was not focused on the LPA branching pattern of the interlobar portion including the relationship with A1 + 2c, lingular arteries, and A6. We analyzed this portion precisely, because knowledge of the relation between the branching pattern of the upper lobe PA branches and A6 is important for surgical resection. Generally speaking in upper or lower lobectomy, as the fissure dissection proceeds, the A6 from the posterolateral surface of the LPA of the interlobar portion is present at a slightly lower level than A1 + 2c to the left upper lobe [1]. Fourdrain et al. [8] evaluated the branching pattern of PA using 3D-CTPA in 44 patients and reported that the origin of A6 as the left lower lobe artery is frequently proximal to the origin of PI (65.9%). To the best of our knowledge, no report has referred to the detailed relationship between A1 + 2c, lingular arteries and A6 of the left interlobar portion.

In the present study, we could diagrammatize the LPA branching pattern of the interlobar portion according to a broad classification in the order of bifurcation from proximal to distal into seven types. The results showed that Type 1 was most frequent 37.5% (120/320). Among the detailed branching patterns, "Yamashita's prevailing pattern," that is, from A1 + 2c, a A6, to a PI in the order and the simplest Type 1, was seen in 48 cases (15.0%) and was the most common

Fig. 5 Detailed branching patterns of each of the seven broad classification types of the LPA branching pattern of the interlobar portion. *PI* the lingular artery from pars interlobaris. **a** Details of branch numbers and positions of Type 1. Each row shows number, position, and frequency of respective patterns. **b** Details of branch numbers and positions of Type 2. Each row shows number, position, and frequency of respective patterns. **c** Details of branch numbers and positions of Type 3. Each row shows number, position, and frequency of respective patterns. **d** Details of branch numbers and positions of Type 4. Each row shows number, position, and frequency of respective patterns. e details of branch numbers and positions of Type 5. Each row shows number, position, and frequency of respective patterns. Only in this type, left axis represents the number of A1 + 2c or A3a of the LPA branching pattern of the interlobar portion, because Type 5 has no PI. f details of branch numbers and positions of Type 6. Each row shows number, position, and frequency of respective patterns. g details of branch numbers and positions of Type 7. Each row shows number, position, and frequency of respective patterns. *S* superior, *I* inferior, *PI* lingular artery that originates from pars interlobaris, and PI´: PI originated from lower portion that is from A8 or the common trunk of A8 and A9

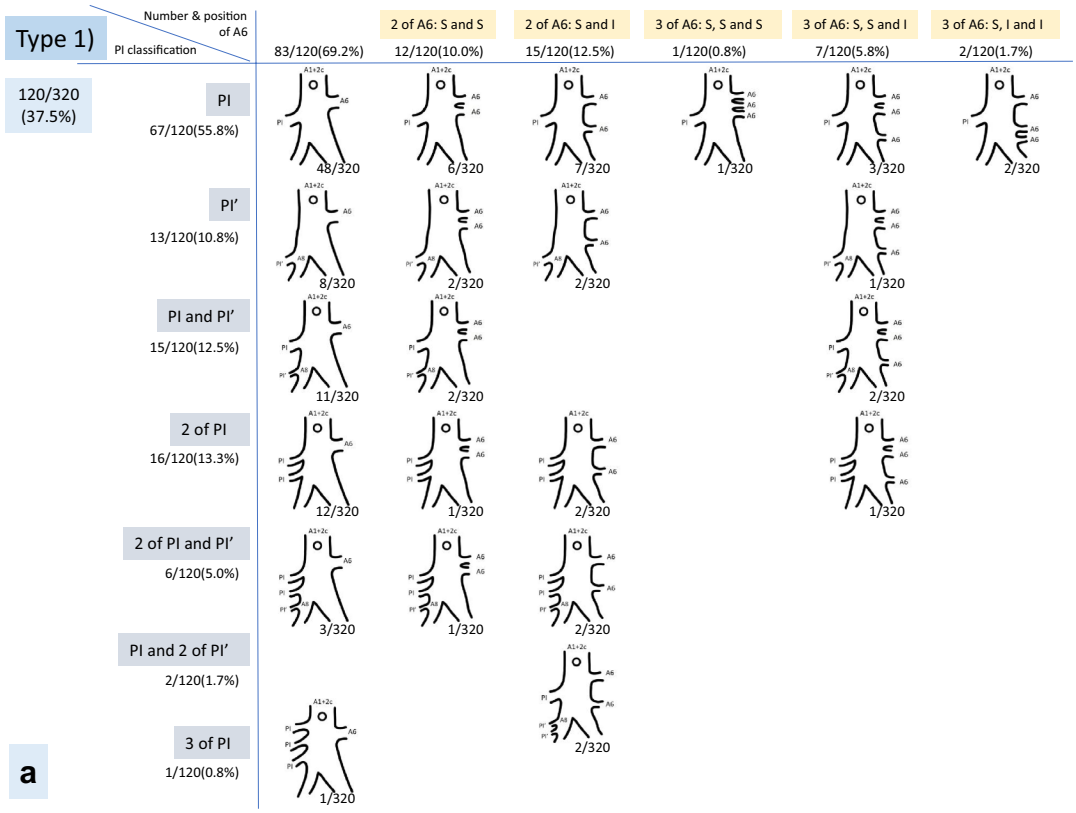
Type 1)
Number & position of A6
PI classification
83/120(69.2%)
2 of A6: S and S
12/120(10.0%)
2 of A6: S and I
15/120(12.5%)
3 of A6: S, S and S
1/120(0.8%)
3 of A6: S, S and I
7/120(5.8%)
3 of A6: S, I and I
2/120(1.7%)
120/320 (37.5%)
PI
67/120(55.8%)
PI'
13/120(10.8%)
PI and PI'
15/120(12.5%)
2 of PI
16/120(13.3%)
2 of PI and PI'
6/120(5.0%)
PI and 2 of PI'
2/120(1.7%)
3 of PI
1/120(0.8%)
a

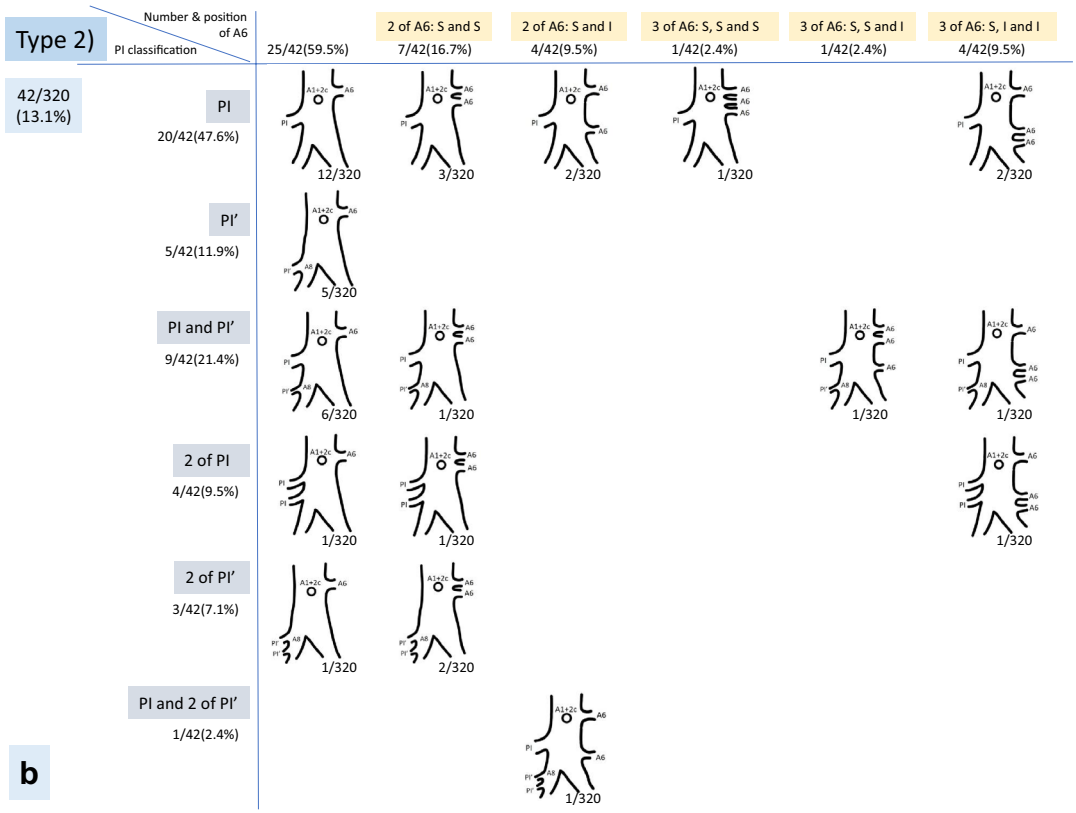
Type 2)
Number & position of A6
PI classification
25/42(59.5%)
2 of A6: S and S
7/42(16.7%)
2 of A6: S and I
4/42(9.5%)
3 of A6: S, S and S
1/42(2.4%)
3 of A6: S, S and I
1/42(2.4%)
3 of A6: S, I and I
4/42(9.5%)
42/320 (13.1%)
PI
20/42(47.6%)
PI'
5/42(11.9%)
PI and PI'
9/42(21.4%)
2 of PI
4/42(9.5%)
2 of PI'
3/42(7.1%)
PI and 2 of PI'
1/42(2.4%)
b

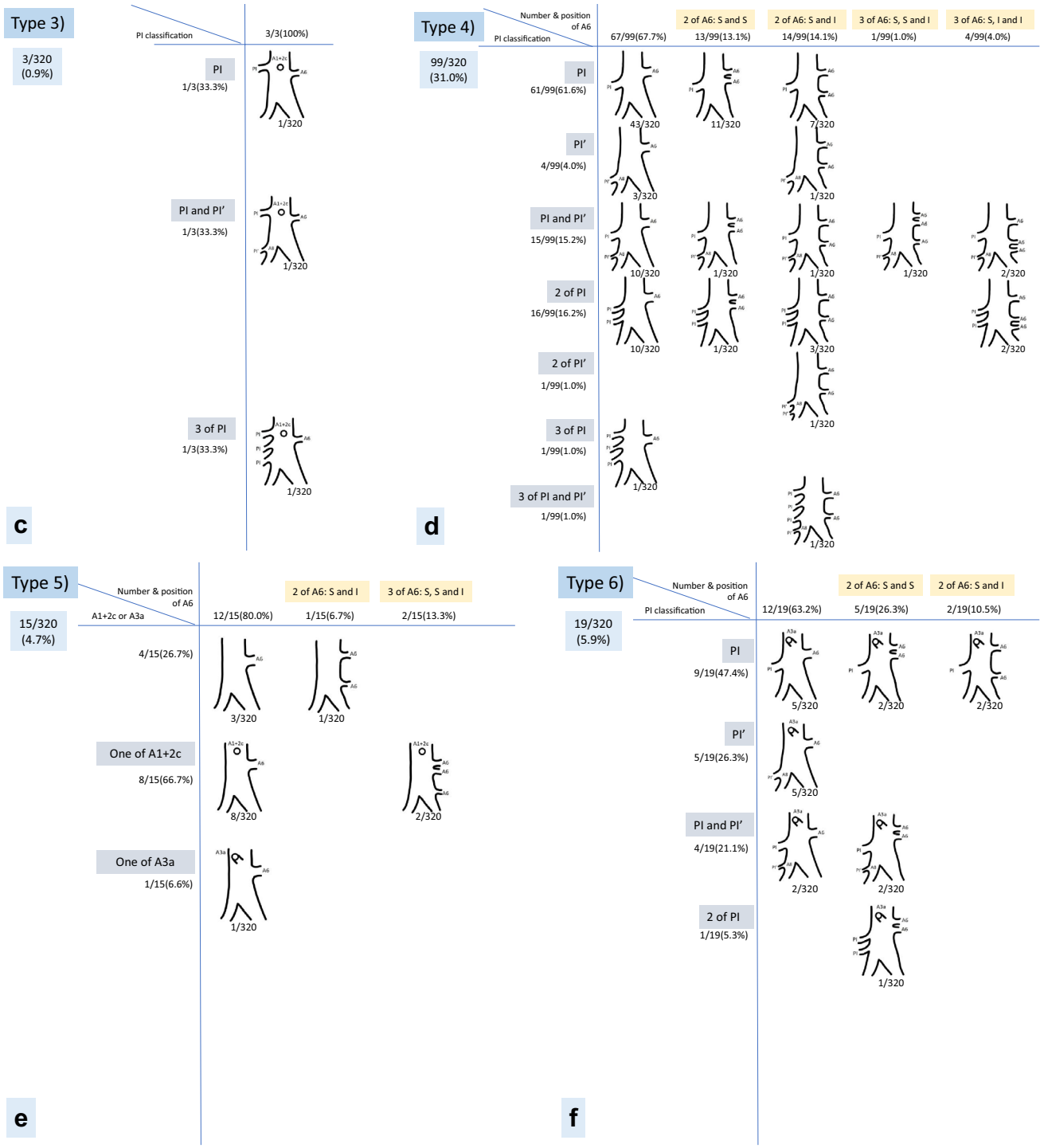

Fig. 5 (continued)

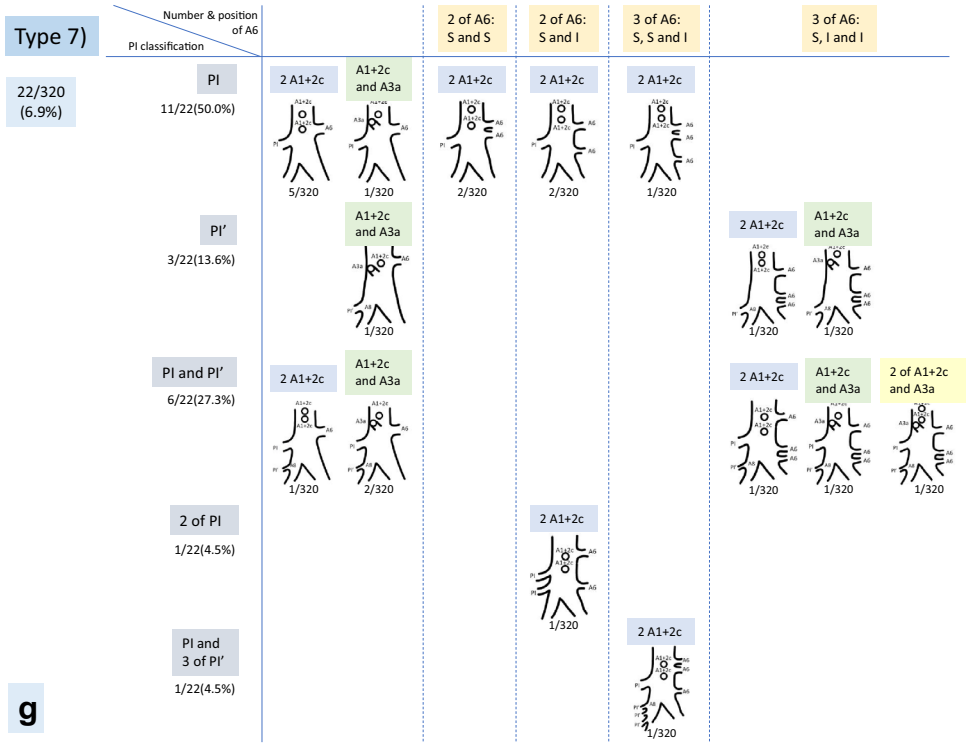

Fig. 5 (continued)

type. Recently, anatomic segmentectomy which preserves more lung function compared to lobectomy is increasingly used to resect lung nodules. However, a segmentectomy is technically more difficult than a standard lobectomy because of the anatomical complexity of the lung, featuring both vascular and bronchial structures that vary at different levels [7]. The thoracoscopic approach is also used for anatomic segmental resection. VATS requires a more detailed understanding of local anatomy than does conventional open surgery [11]. In the present study, we could diagrammatize the LPA branching pattern of the interlobar portion into 85 types in all 320 patients. However, there are many patterns of PA branching, and knowledge and information about the precise pulmonary arterial branching patterns, including rare anatomical variations, and a full understanding of individual anatomy is important for surgeons. The most commonly performed segmental resections are upper division segmentectomy, lingular segmentectomy, S6 segmentectomy, and basilar segmentectomy [17]. Therefore, knowledge of the origin and division of each branch is essential. For example, in the present study, A3a arose from PI in 26 cases (8.1%), A1 + 2c from PI in 12 cases (3.8%), A3a from A1 + 2c in two cases (0.6%), and A3a from A8 in one case (0.3%). If upper division segmentectomy or lingular segmentectomy is performed, these branching patterns need to be distinguished carefully. When upper division segmentectomy is performed in the case of A3a arising from PI, A3a should be resected without resecting PI. Regarding the branching pattern of the lingular arteries (A4 and A5), it is important to recognize whether A4 and A5 arise as PM in addition to PI. In the present study, Type 5, only PM, was seen in only 4.7% of cases, as compared to 9.7% in a previous analysis by Yamashita [15]. It was also reported that PI originates from the lower portion, that is, from A8 or the common trunk of A8 and A9 (PI´) in 95 cases (29.7%), as compared to 4.2% [15]. Several articles have referred to that branching pattern [6, 15, 18], but none have described its frequency by using CT images. This might be dependent on differences between anatomical and radiological evaluations whereby CT images may enable investigation of thinner branches. The identification of PI´ is important. When left lower lobectomy/basilar segmentectomy is performed, PI´ should not be sacrificed. If this variation is encountered, the branches of the lingular artery must be managed separately. Therefore, the relatively high frequency of PI´, approximately 30%, needs to be recognized.

In the case of S3 or S1 + 2 segmentectomy, it is needed to observe whether A1 + 2 or A3a directly originated from the LPA of the interlobar portion. In the present study, Type 6, where A3a directly originated from the LPA of the interlobar portion, was seen in 5.9% (19/320) of the cases. In Type 7, the case of two branches of A1 + 2c directly originated from the LPA of the interlobar portion was found in

15 cases (4.7%), A1 + 2c and A3a directly originated from the LPA of the interlobar portion in six cases (1.9%), and two branches of A1 + 2c and A3a directly originated from the LPA of interlobar portion in one case (0.3%).

In the case of S6 segmentectomy, it is important to identify how many branches there are and where A6 originate from. The second or third branch of A6 may arises from the basal PA which is located lower than that from the LPA of the interlobar portion. We found four branches of A6 in three cases (0.9%), and to the best of our knowledge, there is no other such report.

For precise identification of the anatomical structures, not only 3D-CTPA but also thin-section CT images appears to contribute more to a better evaluation of the smaller PA branches. In a previous study, 99.7% of PA branches were identified on thin-section CT and MPR images, and 8 vessels which were missed on 3D-CTPA could be detected on thin-section MPR images [13]. Identification of sub-subsegmental (i.e., fifth order) PA could also be visualized using thin-section CT and MPR images [19]. Therefore, we emphasize the importance of observing both 3D-CTPA and thin-section CT images. Although perioperative complications and mortality with VATS lobectomy have been reported to occur at frequencies of 5–32% and 0–7%, respectively, postoperative complications in patients undergoing 3D-CTPA imaging were reported in 8% of cases with no mortality [6]. In the present study, postoperative complications occurred in 16.5% with no mortality. The frequency of conversion from VATS lobectomy to open thoracotomy because of vessel bleedings has been reported in 4% of cases [6]. In the present study, the occurrence was 3.7%.

The present study had several limitations: First, it was a retrospective study, which introduced an inherent selection bias. Second, a 64-slice MDCT and a 256-slice MDCT scanners were used. We analyzed the LPA branching pattern of the interlobar portion using 3D-CTPA and thin-section CT images using two CTPA protocols. However, we consider any differences in them not to have affected the results, because CT images are sufficient to investigate the PA branching pattern. Finally, we used 3D-CTPA images and thin-section CT images exclusively. It is possible that these may vary somewhat from the actual anatomical findings. As previous study has shown, there was a good correlation between CT appearance and pathological findings of the segmental abnormalities in the lung [20]. Several research groups have reported that 95–98.7% of PA branches were preoperatively identified using 3D-CTPA [4, 6, 7, 9, 11, 13]. Moreover, 99.7% of PA branches were identified on thin-section MPR images [13]. We think that it was reasonable to analyze the LPA branching pattern of the interlobar portion using 3D-CTPA and thin-section CT images. The above-mentioned previous reports, however, evaluated PA branches of the various lobes together in both lungs or right upper lobe. Comparisons of the findings of 3D-CTPA/thin-section CT images with the intraoperative findings, focusing on the PA branching pattern of the left lobe alone in a relatively large patient population, will be needed in the future.

In conclusion, in the present study, 3D-CTPA and thin-section images provided precise preoperative information regarding PA branching pattern of left interlobar portion. This work is the first to diagrammatize the LPA branching pattern of the interlobar portion and their broad classification into seven types, followed by their precise subclassification into 85 types in all 320 patients. It is necessary to assess the PA branches of the left lobe while also taking into consideration branches supplied from other segments or portions. We believe that the present PA data and diagrammatized patterns will be of value by contributing to the safety and ease of anatomical left upper/lower lobectomy and segmentectomy.

Compliance with ethical standard

Conflicts of interest None declared.

Informed consent The Ethics Committee of Kagawa University Hospital approved this retrospective study and waived the need for obtaining the consent of individual patients.

References

1. Veeramachaneni NK. Surgical anatomy of the lungs. In: LoCicero J, Feins RH, Colson YL, Rocco G, editors. Shields' general thoracic surgery. 8th ed. Philadelphia: Lippincott Williams & Wilkins; 2018. p. 101–111.
2. Kandathil A, Chamarthy M. Pulmonary vascular anatomy & anatomical variants. Cardiovasc Diagn Ther. 2018;8:201–7.
3. Ikeda N, Yoshimura A, Hagiwara M, Akata S, Saji H. Three dimensional computed tomography lung modeling is useful in simulation and navigation of lung cancer surgery. Ann Thorac Cardiovasc Surg. 2013;19:1–5.
4. Akiba T, Marushima H, Harada J, Kobayashi S, Morikawa T. Importance of preoperative imaging with 64-row three-dimensional multidetector computed tomography for safer video-assisted thoracic surgery in lung cancer. Surg Today. 2009;39:844–7.
5. Oizumi H, Kanauchi N, Kato H, Endoh M, Suzuki J, Fukaya K, et al. Anatomic thoracoscopic pulmonary segmentectomy under 3-dimensional multidetector computed tomography simulation: a report of 52 consecutive cases. J Thorac Cardiovasc Surg. 2011;141:678–82.
6. Hagiwara M, Shimada Y, Kato Y, Nawa K, Makino Y, Furumoto H, et al. High-quality 3-dimensional image simulation for pulmonary lobectomy and segmentectomy: results of preoperative assessment of pulmonary vessels and short-term surgical outcomes in consecutive patients undergoing video-assisted thoracic surgery. Eur J Cardiothorac Surg. 2014;46:e120–e126126.
7. Nagashima T, Shimizu K, Ohtaki Y, Obayashi K, Kakegawa S, Nakazawa S, et al. An analysis of variations in the bronchovascular pattern of the right upper lobe using three-dimensional CT

angiography and bronchography. GenThoracCardiovascSurg. 2015;63:354–60.
8. Fourdrain A, De Dominicis F, Blanchard C, Iquille J, Lafitte S, Beuvry P-L, et al. Three-dimensional CT angiography of anatomic variations in the pulmonary arterial tree. Surg Radiol Anat. 2018;40:45–53.
9. Watanabe S, Arai K, Watanabe T, Koda W, Urayama H. Use of three-dimensional computed tomographic angiography of pulmonary vessels for lung resections. Ann Thorac Surg. 2003;75:388–92.
10. Nakamoto K, Omori K, Nezu K. Lung Cancer Project Group of West-Seto Inland Sea J. Superselective segmentectomy for deep and small pulmonary nodules under the guidance of three-dimensional reconstructed computed tomographic angiography. Ann Thorac Surg. 2010;89:877–83.
11. Fukuhara K, Akashi A, Nakane S, Tomita E. Preoperative assessment of the pulmonary artery by three-dimensional computed tomography before video-assisted thoracic surgery lobectomy. Eur J Cardiothorac Surg. 2008;34:875–7.
12. Duong PA, Ferson PF, Fuhrman CR, McCurry KR, Lacomis JM. 3D-multidetector CT angiography in the evaluation of potential donors for living donor lung transplantation. J Thorac Imaging. 2005;20:17–23.
13. Murota M, Yamamoto Y, Satoh K, Ishimura M, Gotoh M, Nishiyama Y. Preoperative evaluation of the right upper lobe pulmonary artery by 3D-CT pulmonary angiography vs. thin-section multiplanar reconstruction images obtained by contrast-enhanced multidetector-row CT. Acta Med Okayama. 2015;69:327–32.
14. Dindo D, Demartines N, Clavien PA. Classification of surgical complications: a new proposal with evaluation in a cohort of 6336 patients and results of a survey. Ann Surg. 2004;240:205–13.
15. Yamashita H. Variations in the pulmonary segments and the bronchovascular trees. In: Roentgenologic anatomy of the lung. Tokyo: Igaku-Shoin; 1978. pp. 70–107.
16. Topol M. Place of origin of the apical segmental artery of the left inferior lobe in relation to other branches arising from the interlobar portion of the left pulmonary artery in human. Folia Morphol. 1996;55:175–85.
17. Pan X, Zhang Y, Ren S, Ding Z, Li X, Zhu D, et al. Video-assisted thoracoscopic superior segmentectomy of the right lower lobe. J Thorac Dis. 2016;8:1349–52.
18. Gossot D, Seguin-Givelet A. Anatomical variations and pitfalls to know during thoracoscopic segmentectomies. J Thorac Dis. 2018;10:S1134–S1144144.
19. Murota M, Satoh K, Yamamoto Y, Kobayashi T, Nishiyama Y. Evaluation of subsubsegmental pulmonary arteries of the posterior and anterior segments of the right upper lobe using multidetector row computed tomography with multiplanar reconstruction images. Jpn J Radiol. 2009;27:86–90.
20. Otsuji H, Uchida H, Maeda M, Iwasaki S, Yoshiya K, Hatakeyama M, et al. Incomplete interlobar fissures: bronchovascular analysis with CT. Radiology. 1993;187:541–6.